

## Magnetic Pomegranate Peel Extracts Modified Iron Oxide Nanocatalyst for Green and Selective Oxidation of Benzyl alcohols

Sheyda Iranfar<sup>a</sup>, Hakimeh Ziyadi<sup>a\*</sup>, Malak Hekmati<sup>a</sup>, Ensieh Ghasemi<sup>b</sup>, Davoud Esmaili<sup>c</sup>, Pegah Haghghi<sup>d</sup>

a) Department of Organic Chemistry, Faculty of Pharmaceutical Chemistry, Tehran Medical Sciences, Islamic Azad University, Tehran, Iran.

b) Department of chemistry, Faculty of pharmaceutical Chemistry, Tehran Medical Sciences, Islamic Azad University, Tehran, Iran.

c) Department of Microbiology and Applied Virology Research Center, Baqiyatallah University of Medical Sciences, Tehran, Iran.

d) Active Pharmaceutical Ingredients Research Center, Tehran Medical Sciences, Islamic Azad University, Tehran, Iran.

Received 25 June 2021; received in revised form 18 November 2021; accepted 5 December 2021

### ABSTRACT

The preparation and application of novel nanocatalysts for oxidation reaction via a simple, effective, green method remains a challenge; thus, in this study, a facile and eco-friendly approach is suggested to fabricate pomegranate peel extract (PPE) functionalized on silicate-coated Fe<sub>3</sub>O<sub>4</sub> nanoparticles (Fe<sub>3</sub>O<sub>4</sub>@SiO<sub>2</sub>-PPE). The physicochemical characteristics of the magnetic Fe<sub>3</sub>O<sub>4</sub>@SiO<sub>2</sub>-PPE nanocomposite were evaluated using Fourier-transform infrared spectroscopy (FT-IR), X-ray diffraction (XRD), scanning electron microscopy (SEM), and transmission electron microscopy (TEM) techniques. SEM images showed well-distributed nanoparticles in shape and size with a mean diameter of 42 nm. FT-IR and TEM images proved appropriate functionalization with pomegranate peel extract. The Fe<sub>3</sub>O<sub>4</sub>@SiO<sub>2</sub>-PPE nanocatalyst was found to be useful in the selective oxidation of benzyl alcohols to the relevant aldehydes/ketones without significant over oxidation and with good-to-excellent (about 95%) yields under solvent-free conditions at room temperature. The results revealed that the prepared catalyst was easily recovered and reused for five consecutive oxidation cycles without losing selectivity towards desired products in the benzyl alcohol oxidation.

**Keywords:** Pomegranate peel extract, Iron oxide nanoparticle, Catalyst, Oxidation.

### 1. Introduction

The catalytic oxidation of alcohols to their corresponding carbonyl compounds is a vital reaction for both scientific research and industries [1-3]. Generally, the selective oxidation of alcohols to ketones or aldehydes without any unwanted byproducts is significant for the synthesis of various precious chemicals such as pharmaceuticals and the development of environment-friendly energy resources [4-7]. Over the past decades, great efforts have been made to fabricate and develop beneficial catalysts for such processes.

\*Corresponding author:

E-mail address: [behnazziyadi@yahoo.com](mailto:behnazziyadi@yahoo.com) (H. Ziyadi)

Thus far, numerous noble metal-based catalysts such as gold, palladium, and platinum have been used, showing excellent selectivity in these transformations [8-12]. The use of these noble metal-based catalysts has been limited due to the high price, unavailability on a large scale, and insufficiency of resources [13-14]. Hence, there has been a growing demand for cost-effective and eco-friendly catalysts with suitable selectivity towards the desired compounds. In recent years, transition metal-based catalysts (Co, Mn, Mo, Fe, Cu, etc.) have attracted considerable attention for the selective oxidation of alcohols [15-19]. Ghasempour and coworkers synthesized and characterized a novel Fe trimer (Fe<sub>3</sub>O) based MOF (Fe-MOF) that promotes benzyl alcohol

oxidation with excellent selectivity toward benzaldehyde [20].

In comparison to noble metal-based catalysts, the lower selectivity and reactivity of first-row transition metal-based catalysts results in their limited application [21]. Additionally, there are still various challenges such as the employment of toxic and hazardous oxidant agents to enhance the reactivity in reactions and some disadvantages such as uneconomical operational prices, generation of unsafe wastes, and unwanted byproducts.

Some outstanding alternatives for the above-mentioned concerns include using green oxidants such as air, hydrogen peroxide ( $H_2O_2$ ), molecular oxygen and carbon dioxide to provide moderate reaction conditions for the environmentally benign oxidation of alcohols [19, 22-25]. For instance, Meng et.al used decacarbonyl dimanganese  $Mn_2(CO)_{10}$  as a catalyst to aerobic oxidation of alcohols with air [24]. Cu doped  $SrTiO_3$  was synthesized and was investigated as the photocatalyst for selective alcohol oxidation under mild conditions [19]. Moreover, Wang et.al showed that a pure inorganic ligand-supported chromium compound ( $(NH_4)_3[CrMo_6O_{18}(OH)_6]$ ) could be used to effectively promote this type of reaction in the presence of  $CO_2$  [25]. Nevertheless, most of these liquid-phase oxidation processes were performed in different toxic organic solvents such as acetonitrile, dimethyl sulfoxide, or toluene, which is not in line with the green chemistry. Therefore, designing and fabricating novel heterogeneous nanocatalysts for the green, selective oxidation of alcohols is of high significance in both green and organic chemistry.

Recently, the design and synthesis of magnetic bio-nanocatalysts based on biocompatible and natural compounds have captured researchers' attention in the field of green chemistry [26-27]. Magnetic nanoparticles (MNPs) have received great attention in a wide range of applications such as biomedical applications, magnetic resonance imaging (MRI), environmental remediation bio-separation, and especially heterogeneous catalysis because of their low toxicity, high catalytic activity, moisture and air tolerance, ease of separation, recyclability, low corrosion, and environmental (eco-friendly) concepts [28-31]. Of different the kinds of MNPs, magnetic  $Fe_3O_4$  NPs is widely employed in the structure of Fenton-like heterogeneous catalysts for oxidation reaction [32-35].

Tending to agglomerate, the modification of the magnetic core is critical for protection in the case of oxidation and particle agglomeration. Consequently, the convenient surface modification of iron oxide NPs

(IONPs) is required to make resistant, biocompatible, less toxic, thermal and mechanical resistance [36]. Various polymers, carbon materials, natural compounds, and silica are suitable for fabricating biocompatible magnetic composites. Silica is one of the most widely employed reagents for modifying the surface of IONPs [37, 38]. Silica coating not only suppresses the aggregation of IONPs but also enhances their mechanical and chemical stability, providing a new substrate for further functionalization. By so doing, it makes them a promising candidate in the catalysis field. Kannappan et. al synthesized polyamine dendrimer stabilized gold nanoparticles with core of  $Fe_3O_4@SiO_2$  by a difficult modification method and this was employed as the green catalyst for the selective oxidation of benzyl alcohol to aldehyde in presence of oxygen and toluene as oxidant and solvent respectively [39]. The additional functionalization of IONPs with biomolecules and plant extract, as an easy process, has numerous advantages from a green chemistry point of view. Moreover, bio-functionalization could improve surface properties of IONPs by inserting compounds with catalytic properties, such as oxidizing agents, in plant extracts.

*Punica Granatum* peel or pomegranate peel is a novel source of bioactive secondary metabolites with many biological activities such as antioxidant and anti-cancer properties [40-42]. *Punica Granatum* peel is a rich source of various types of flavonoids, anthocyanins, and tannins used as stabilizing and capping reagents in the green synthesis of several metals and metal oxide NPs [43-46]. Due to being a rich source of hydroxyl and phenolic groups, the application of pomegranate peel extract makes it a promising and efficient green catalyst for the oxidation reaction of benzyl alcohols.

Given the above-mentioned arguments, in this study, we report a cost-effective and facile approach for the preparation of a novel nanocatalyst based on pomegranate peel extract modified by silica-coated  $Fe_3O_4$  NPs ( $Fe_3O_4@SiO_2$ -PPE) for the selective oxidation of benzyl alcohols to corresponding carbonyl compounds. Furthermore, the proposed nanocatalyst can be magnetically separated from the reaction medium and reused several times without producing hazardous wastes.

## 2. Experimental

### 2.1. Materials and instrumentation

Pomegranate fruits were purchased from the local market. All other chemicals and materials were obtained from Merck Company and used without any further purification processes. All the organic products were

known compounds characterized by IR, Mass,  $^1\text{H}$ NMR spectroscopic data and compared with those reported in the literature [16-19]. The Fourier transform infrared spectra were obtained over the region of  $400\text{-}4000\text{ cm}^{-1}$  with a Perkin Elmer Spectrum two FT-IR and spectroscopic grade KBr. The transmission electron microscopy (TEM) images of magnetic  $\text{Fe}_3\text{O}_4@\text{SiO}_2$ -PPE nanocatalyst were also recorded applying a Zeiss-EM10C transmission microscope. SEM images were observed using SEM (Philips XL 30 and S-4160) with a gold coating. The graph of the distribution of nanoparticles was drawn by measurement and Origin 8.6 software based on 20 nanoparticles at random in the SEM image. Powder XRD spectrum was recorded at room temperature by a Philips X'pert 1710 diffractometer using  $\text{Co K}\alpha$  ( $\alpha = 1.54056\text{ \AA}$ ) in Bragg-Brentano geometry ( $\theta$ - $2\theta$ ) to investigate the crystallographic phase and purity of the prepared magnetic nanocatalyst.

### 2.2. Preparation of pomegranate peel extract (PPE)

Fresh pomegranate peels were collected and rinsed with deionized water; they were then cut into small pieces. Next, 10 g of pomegranate peels was heated with 100 ml deionized water at  $60\text{ }^\circ\text{C}$  for 1 h and then cooled at room temperature. The obtained mixture was filtered with a filter paper, and the final extract was collected and stored at  $4\text{ }^\circ\text{C}$  for subsequent experiments.

### 2.3. Magnetic iron oxide preparation

$\text{Fe}_3\text{O}_4$  NPs were first synthesized by the chemical coprecipitation approach reported by Sun et. al. [47]. Accordingly, a solution of 20 mmol  $\text{FeCl}_2$  and 20 mmol  $\text{FeCl}_3\cdot 6\text{H}_2\text{O}$  in 40 mL deionized water was initially prepared by mechanical stirring. To stir the solution vigorously, 10 mL  $\text{NH}_3$  was added drop wise until the pH reached 12, and a black particulate was produced subsequently. Next, the mixture was refluxed at  $150\text{ }^\circ\text{C}$  for 1 hour. Afterward, 80 mL ethanol and 20 mL TEOS were carefully introduced to the solution and then stirred at  $40\text{ }^\circ\text{C}$  for 24 hours. Finally, the fabricated  $\text{Fe}_3\text{O}_4@\text{SiO}_2$  nanoparticles were separated magnetically and washed one time with diethyl ether and washed three times with water and ethanol solution (1:1 V/V). The as-prepared  $\text{Fe}_3\text{O}_4@\text{SiO}_2$  nanoparticles were vacuum-dried at  $100\text{ }^\circ\text{C}$  for 24 hours.

### 2.4. Preparation of $\text{Fe}_3\text{O}_4@\text{SiO}_2$ nanoparticles modified with pomegranate peel extract ( $\text{Fe}_3\text{O}_4@\text{SiO}_2$ -PPE)

First, 2 g of the obtained  $\text{Fe}_3\text{O}_4@\text{SiO}_2$  nanoparticles were added into pomegranate peel aqueous extract (50 mL) and stirred for 1 hour at  $50\text{ }^\circ\text{C}$ . Next, the obtained suspension was stirred at room temperature for 24 hours

to form a paste-shaped material. Afterward, the prepared sample was oven-dried at  $50\text{ }^\circ\text{C}$  for 3 hours.

### 2.5. General procedure for catalytic oxidation of alcohols

The catalytic performance of the  $\text{Fe}_3\text{O}_4@\text{SiO}_2$ -PPE nanocatalyst was investigated in selective oxidation of different alcohols. Alcohol (1 mmol) and 10 mg of  $\text{Fe}_3\text{O}_4@\text{SiO}_2$ -PPE were added to a round-bottom, two-necked flask under reflux and solvent-free conditions. Then,  $\text{H}_2\text{O}_2$  (30%) was added slowly, and the mixture was stirred for 10 min. Then, the reaction mixture was cooled at room temperature and stirred for 2 h. Finally, the magnetic nanocatalyst was recovered by a small magnet. The progress of the alcohol oxidation reaction was evaluated by thin-layer chromatography (TLC). Finally, the structural characteristics of the obtained products were characterized by FT-IR,  $^1\text{H}$  NMR, and MASS spectrometry analyses.

## 3. Results and Discussion

### 3.1. $\text{Fe}_3\text{O}_4@\text{SiO}_2$ -PPE nanocatalyst preparation and characterization

The main aim of this study was to design and develop a novel magnetically separable nanocatalyst based on a further surface modification of  $\text{Fe}_3\text{O}_4@\text{SiO}_2$  nanoparticles with pomegranate peel extract [48]. To characterize the functional groups of the synthesized samples, FT-IR spectra of pomegranate peel extract,  $\text{Fe}_3\text{O}_4@\text{SiO}_2$  nanoparticles, and  $\text{Fe}_3\text{O}_4@\text{SiO}_2$ -PPE are presented in **Fig. 1**. A sharp peak at  $3400\text{ cm}^{-1}$  shows the vibrations of the hydroxyl group of flavonoids and phenolic compounds present in pomegranate peel aqueous extract as well as a silica coating.

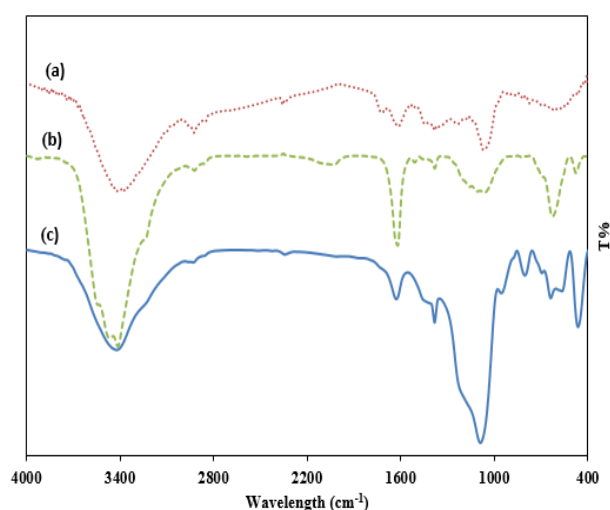


**Fig. 1** FT-IR spectra of (a) pomegranate peel extract (b)  $\text{Fe}_3\text{O}_4@\text{SiO}_2$  and (c)  $\text{Fe}_3\text{O}_4@\text{SiO}_2$ -PPE NP

According to **Fig. 1 (a)**, the absorption bands appeared at 3400 and 1610  $\text{cm}^{-1}$ , corresponding to the O-H stretching and bending vibrations of phenolic and flavonoid secondary metabolites in *Punica Granatum* extract. As depicted in **Fig. 1 (b)**, two absorption bands at 479 and 629  $\text{cm}^{-1}$  were attributed to the Fe-O bond in magnetic iron oxide nanoparticles [49]. The observed absorption bands at 950 and 1080  $\text{cm}^{-1}$  are the important characteristics of the Si-OH and Si-O-Si bond respectively in silica-coated magnetic nanoparticles [42]. FT-IR analyses propose that the pomegranate peel extract functionalized successfully on the  $\text{Fe}_3\text{O}_4@\text{SiO}_2$  nanoparticles. The appearance of the new band at 1380  $\text{cm}^{-1}$  of **Fig. 1 (c)** can be attributed to C-O stretching vibration, related to the involvement of C-O groups of biomolecules of PPE extract in the synthesis of  $\text{Fe}_3\text{O}_4@\text{SiO}_2$ -PPE nanoparticles. It is suggested that the pomegranate peel extract (PPE) bonds interact with  $\text{Fe}_3\text{O}_4@\text{SiO}_2$  via hydrogen bonding. FT-IR spectra show that the bonding density of Si-OH at 950  $\text{cm}^{-1}$  for  $\text{Fe}_3\text{O}_4@\text{SiO}_2$  shifted to a lower frequency at 803  $\text{cm}^{-1}$  for  $\text{Fe}_3\text{O}_4@\text{SiO}_2$ -PPE demonstrating the interaction between extract and the nanoparticles. Also it should be noted that a small amount of explanation and frequency shifts in OH peak at 3400  $\text{cm}^{-1}$  was observed.

**Figs. 2 (a) and (b)** represent the X-ray diffraction (XRD) patterns of  $\text{Fe}_3\text{O}_4@\text{SiO}_2$  and  $\text{Fe}_3\text{O}_4@\text{SiO}_2$ -PPE magnetic nanoparticles, respectively. As observed in **Fig. 2 (a)**, the peaks at  $2\theta$  30.36°, 36.08°, 43.57°, 53.43°, 57.61° and 63.01° can be related to (220), (311), (422), (400), (511) and (540) Bragg reflections, respectively, which accorded well with the standard cubic spinel structure of  $\text{Fe}_3\text{O}_4$  (reference JCPDS card no. 19-629) [47]. Furthermore, additional peaks appeared at diffraction angles at  $2\theta$  10-20°, corresponding to the amorphous phase of  $\text{SiO}_2$ . The XRD pattern of  $\text{Fe}_3\text{O}_4@\text{SiO}_2$ -PPE nanoparticles, **Fig. 2 (b)**, displayed that introduction of pomegranate peel extract could not affect the crystalline structure of  $\text{Fe}_3\text{O}_4@\text{SiO}_2$  NPs, which indicates the successful surface modification of magnetic NPs.

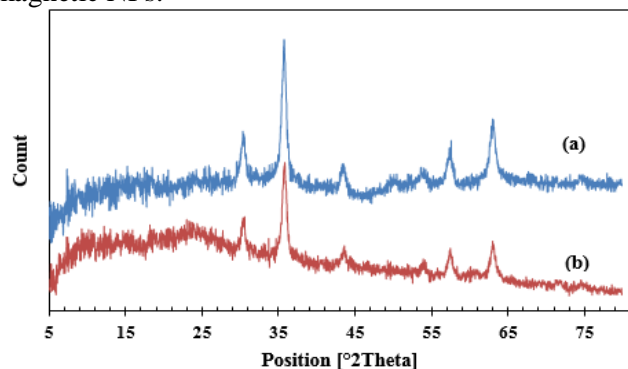


**Fig. 2** XRD pattern of (a)  $\text{Fe}_3\text{O}_4@\text{SiO}_2$  NPs (b)  $\text{Fe}_3\text{O}_4@\text{SiO}_2$ -PPE NPs

The surface morphology and shape of the samples and the histogram of size distribution were studied using SEM images (**Fig. 3**). **Fig. 3 (a)** shows the semi-spherical shape and well-distributed size of  $\text{Fe}_3\text{O}_4@\text{SiO}_2$ -PPE NPs with some agglomeration. The observed agglomeration is due to the presence of pomegranate peel extract metabolites on the NPs surface and the formation of hydrogen bonds. The histogram of size distribution of nanoparticles depicts particles' size, **Fig. 3 (b)** in the range of 21 to 61 nm with a mean diameter of 42 nm. The amount and chemical compositions of the prepared sample were identified using EDX analysis. **Fig. 3 (c)** shows the EDX spectrum of the catalyst and the chemical structure of  $\text{Fe}_3\text{O}_4@\text{SiO}_2$ -PPE consisting of Fe, O, Si, carbon, and nitrogen elements. Silica coating was approved by the existence of Si in EDX analysis. Yet, the presence of carbon and nitrogen shows that the surface of nanoparticles is coated by biomolecules of pomegranate peel extract.

In addition, the morphology and size distributions of  $\text{Fe}_3\text{O}_4@\text{SiO}_2$  nanoparticles modified with pomegranate peel extract were further studied using transmission electron microscopy (TEM). **Fig. 4** depicts that the particles are spherical in shape and uniformly dispersed. Modification with pomegranate peel extract can be approved with the existence of two  $\text{Fe}_3\text{O}_4@\text{SiO}_2$  organic and inorganic phases in the TEM image.

### 3.2. Catalytic activity of $\text{Fe}_3\text{O}_4@\text{SiO}_2$ -PPE magnetic nanocatalyst in the selective oxidation of benzyl alcohol

To investigate the catalytic activity of the magnetic  $\text{Fe}_3\text{O}_4@\text{SiO}_2$ -PPE nanocatalyst, the oxidation of benzyl alcohol was selected as a model reaction (**Scheme 1**). In the common catalysis, benzyl alcohol was transformed into benzaldehyde in the presence of  $\text{H}_2\text{O}_2$ , and the catalytic procedure conditions were optimized; the obtained results are presented in **Table 1**. In line with green chemistry goals, the catalytic oxidation of benzyl alcohol was performed under solvent-free conditions. For optimizing the reaction condition, the effects of different variables such as catalyst amount,  $\text{H}_2\text{O}_2$  amount and time duration were measured (**Table 1**).

In the next step, the catalytic oxidation of benzyl alcohol was carried out at various reaction conditions such as temperature. It can be seen that an increase in reaction temperature from 25 °C (room temp) to 75 °C decreased the product yield. Of note, lower selectivity and yield were obtained when the catalytic oxidation reaction was performed at a higher temperature. The effect of other factors such as time of reaction, amount of catalyst, and

H<sub>2</sub>O<sub>2</sub> were also studied (**Table 1**). According to **Table 1** (entry 1), the best benzaldehyde yield (95 %) was obtained after 2 h in aqueous reaction medium. The amount of magnetic Fe<sub>3</sub>O<sub>4</sub>@SiO<sub>2</sub>-PPE nanocatalyst plays a vital role in catalytic benzyl alcohol conversion. Interestingly, the use of 20 mg Fe<sub>3</sub>O<sub>4</sub>@SiO<sub>2</sub>-PPE as a novel nanocatalyst considerably increased the yield to 92% (**Table 1**, entry 9). The effect and importance of the catalyst role was observed when the oxidation reaction exhibited low yields in

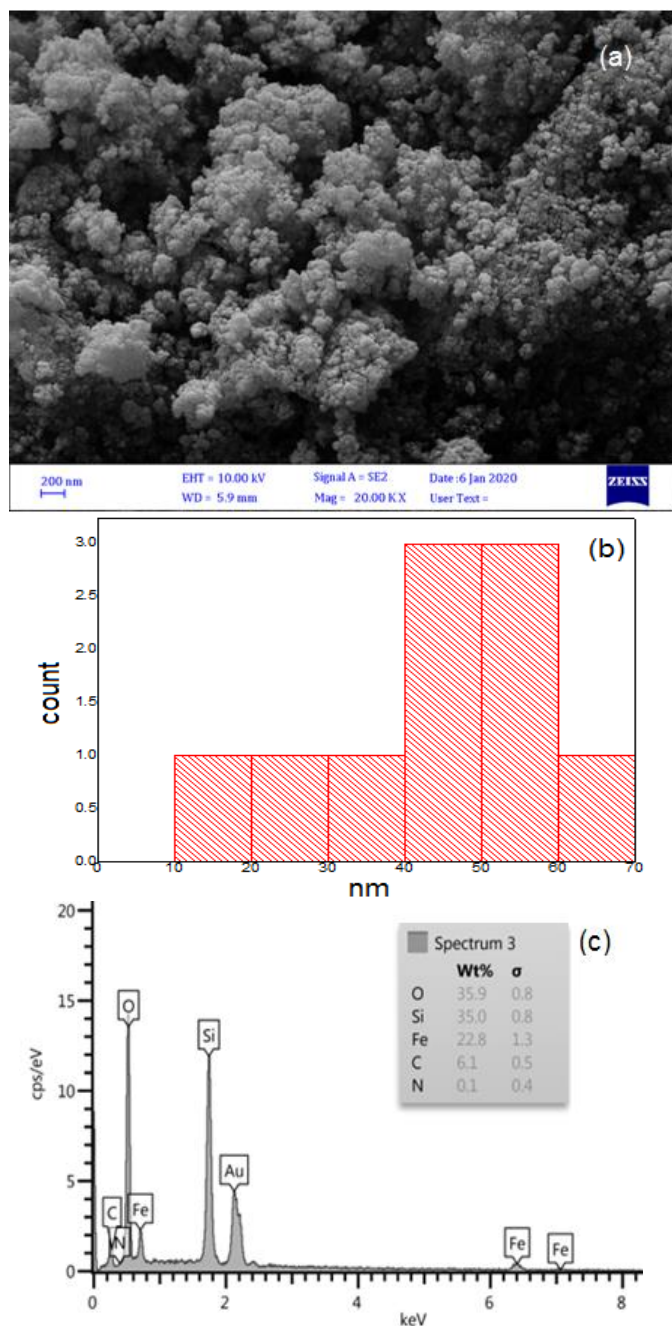


**Fig. 3** (a) SEM micrograph and (b) EDX spectrum of Fe<sub>3</sub>O<sub>4</sub>@SiO<sub>2</sub>-PPE NPs

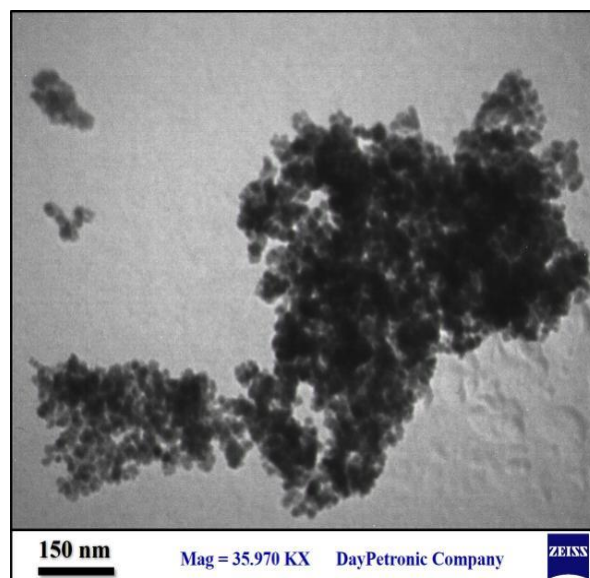
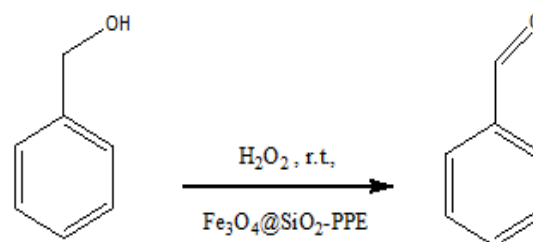


**Fig. 4** TEM image of Fe<sub>3</sub>O<sub>4</sub>@SiO<sub>2</sub>-PPE NPs



**Scheme 1** Oxidation of benzyl alcohol in presence of Fe<sub>3</sub>O<sub>4</sub>@SiO<sub>2</sub>-PPE nanocatalyst

**Table 1** Optimization of oxidation reaction of benzyl alcohol in presence of Fe<sub>3</sub>O<sub>4</sub>@SiO<sub>2</sub>-PPE NP

Entry	Catalyst amount (mg)	Time (h)	Oxidant amount (mmol)	Yield (%)
1	-	6	1	20
2	-	24	1	62
3	10	1	0.5	30
4	10	2	0.5	53
5	10	6	0.5	90
6	10	1	1	84
7	10	2	1	90
8	20	1	1	92
9	20	2	1	95

the absence of Fe<sub>3</sub>O<sub>4</sub>@SiO<sub>2</sub>-PPE (**Table 1**, entry 1, 20%). Furthermore, the amounts of H<sub>2</sub>O<sub>2</sub> were also optimized. The highest yield was obtained in the presence of 1 mmol H<sub>2</sub>O<sub>2</sub> as an effective oxidant at room temperature for 2 h. The best results of benzyl alcohol oxidation were obtained using 20 mg of Fe<sub>3</sub>O<sub>4</sub>@SiO<sub>2</sub>-PPE nanocatalyst, 1 mmol of H<sub>2</sub>O<sub>2</sub> as oxidant, and 1 mmol of benzyl alcohol under solvent-free conditions at room temperature.

The results of benzyl alcohol oxidation with different catalysts have been compared in **Table 2**. As can be seen, oxidation of benzyl alcohol, in the presence of magnetite cored polyamine dendrimer [39], Fe-based MOF [20], Mn<sub>2</sub>(CO)<sub>10</sub> [24], and carbon hybrid supported platinum nanoparticles (Pt@CHs) [10] were performed in different toxic organic solvents such as toluene and acetonitrile (**Table 2**, entry 2, 4, 5 and 6). Pd nanoparticles supported on pyrazolone-functionalized hollow mesoporous silica [12] catalyst need extra amount of oxidant and also, the product had low yield. The same result can be seen in catalytic oxidation using Au-SiO<sub>2</sub> [8]. Generally, high yield, small amount of oxidant and solvent free condition are an advantage of the novel Fe<sub>3</sub>O<sub>4</sub>@SiO<sub>2</sub>-PPE nano catalyst in catalytic benzyl alcohol oxidation.

The reusability of the catalyst was also examined. After completing the first run of model reaction, the catalyst was washed with CH<sub>2</sub>Cl<sub>2</sub> three times and then dried in a

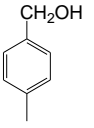
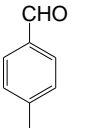
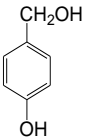
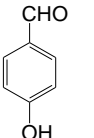
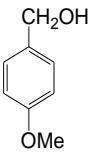
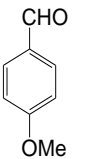
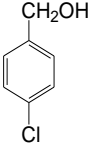
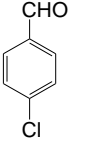
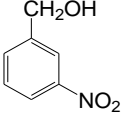
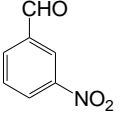
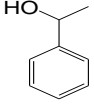
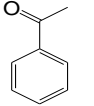
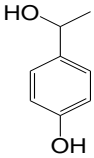
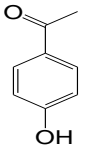
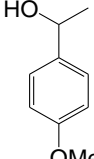
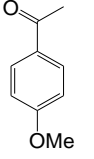
vacuum and reused in the subsequent reaction. The magnetic properties of the catalyst lead to an easy separation process using a magnet. No significant loss of catalyst activity was observed even after 5 times of reuse (**Fig. 5**).

To evaluate the substrate scope, different primary and secondary benzyl alcohols were subjected to oxidation under optimized conditions. The obtained results are summarized in **Table 3**. It seems that the electronic effect of substituents on the aromatic ring is influential in the yield of oxidation reaction. Surprisingly, electron-donating groups such as methoxy or hydroxyl benzaldehydes were obtained as high as 95% in a short time (2 h) (**Table 3**, entries 3 and 4) with a very small amount of over oxidation to corresponding carboxylic acid. However, electron-withdrawing groups such as Cl or NO<sub>2</sub> bearing benzyl alcohol derivatives needed more reaction time or higher catalyst amount and this is not in line with green chemistry guidelines. It can be seen that the prepared nanocatalyst was able to catalyze secondary benzyl alcohol to corresponding ketones more efficiently with high selectivity (**Table 3**, entry 7-9). Consequently, the modified pomegranates peel extract (Fe<sub>3</sub>O<sub>4</sub>@SiO<sub>2</sub> NPs) can be employed as an effective catalyst for the selective oxidation of benzyl alcohol derivatives to their corresponding aldehydes or ketones.

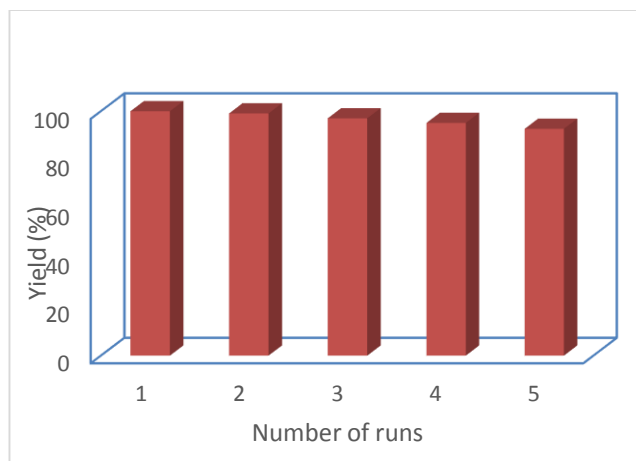
**Table 2** Comparison of different catalyst activity in benzyl alcohol oxidation reaction

Entry	Catalyst	Time (h)	Oxidant	solvent	Yield (%)	Ref.
1	Fe <sub>3</sub> O <sub>4</sub> @SiO <sub>2</sub> -PPE	2	H <sub>2</sub> O <sub>2</sub> (1 eq)	Solvent-free	95	This work
2	magnetite cored polyamine dendrimer (Au@PNPEDA-COOH@Fe <sub>3</sub> O <sub>4</sub> /SiO <sub>2</sub> )	5	O <sub>2</sub>	toluene	87	[39]
3	Pt loaded Cu doped SrTiO <sub>3</sub>	6	air	H <sub>2</sub> O	80.2	[19]
4	Fe-based MOF	3	TBHP	CH <sub>3</sub> CN	91.9	[20]
5	Mn <sub>2</sub> (CO) <sub>10</sub>	12	air	toluene	95	[24]
6	Carbon hybrid supported platinum nanoparticles (Pt@CHs)	3	O <sub>2</sub>	toluene	99	[10]
7	palladium nanoparticles supported on nitrogen-containing ordered mesoporous carbon	3	O <sub>2</sub>	Solvent-free	72	[11]
8	Pd nanoparticles supported on pyrazolone-functionalized hollow mesoporous silica	4	H <sub>2</sub> O <sub>2</sub> (3 eq)	EtOH	70	[12]
9	Au-SiO <sub>2</sub>	6	O <sub>2</sub>	Solvent-free	68.3	[8]

**Table 3** Substrate scope of catalytic oxidation of different aromatic alcohols

Entry	Alcohol	Product	Time (h)	Yield <sup>1</sup>
1			2	95
2			2	92
3			1	95
4			2	95
5			3	84
6			6	80
7			2	79
8			2	89
9			2	83

<sup>1</sup>Reaction conditions: alcohol (1 mmol), H<sub>2</sub>O<sub>2</sub> (1 mmol) Fe<sub>3</sub>O<sub>4</sub>@SiO<sub>2</sub>-PPE (20 mg), room temperature, solvent free.

**Fig. 5** Reusability of Fe<sub>3</sub>O<sub>4</sub>@SiO<sub>2</sub>-PPE NPs in oxidation reaction of benzyl alcohol

#### 4. Conclusions

Pomegranate peel extract (PPE) functionalized on Fe<sub>3</sub>O<sub>4</sub>@SiO<sub>2</sub> nanocomposite (Fe<sub>3</sub>O<sub>4</sub>@SiO<sub>2</sub>-PPE) was successfully prepared by easily available compounds and methods. Analyses such as FT-IR, FE-SEM, EDX, VSM, and BET were carried out for the exact characterization of the prepared nanocatalyst. The Fe<sub>3</sub>O<sub>4</sub>@SiO<sub>2</sub>-PPE nanocatalyst could be recycled several times after a simple and efficient recovery from the reaction medium via an external permanent magnetic field wherein benzyl alcohol was transformed to the corresponding carbonyl products. High-to-excellent yields were obtained for all benzyl alcohol derivatives. High selectivity, low reaction temperature, fast reaction periods, application of green and cheap materials in solvent-free condition, cost-effectiveness, and easy reusability are some of the advantages of the proposed protocol, which makes it a convenient alternative for various benzyl alcohol derivatives, aiming to introduce a novel plant-based catalyst to oxidation industry.

#### Acknowledgements

The authors would like to acknowledge the Active Pharmaceutical Ingredients Research Center (APIRC), Tehran Medical Sciences, Islamic Azad University, for equipment and laboratory services.

#### References

- [1] P. Piotrowski, J. Żukrowski, A. Kaim, *New J. Chem.* 44 (2020) 1971-1978.
- [2] H. Alamgholiloo, S. Rostamnia, K. Zhang, TH. Lee, Y. Lee, R.S. Varma, H.W. Jang, M. Shokouhimehr, *ACS omega.* 5 (2020) 5182-5191.
- [3] X. Yao, C. Bai, J. Chen, Y. Li, *RSC Adv.* 6 (2016) 26921-26928.

- [4] M.N. Kopylovich, A.P. Ribeiro, E.C. Alegria, N.M. Martins, L.M. Martins, A.J. Pombeiro, *Adv. Organomet. Chem.* 63 (2015) 91-174.
- [5] T. Mallat, A. Baiker, *Chem. Rev.* 104 (2004) 3037-3058.
- [6] G.K. Kara, J. Rahimi, M. Niksefat, R. Taheri-Ledari, M. Rabbani, A. Maleki, *Mater. Chem. Phys.* 250 (2020) 122991-123005.
- [7] K. Mori, T. Hara, T. Mizugaki, K. Ebitani, K. Kaneda, *J. Am. Chem. Soc.* 126 (2004) 10657-66.
- [8] E. Hammond-Pereira, K. Bryant, T.R. Graham, C. Yang, S. Mergelsberg, D.Wu, S.R. Saunders, *React. Chem. Eng.* 5 (2020) 1939-1949.
- [9] S. Meher, R.K. Rana, *Green Chem.* 21 (2019) 2494-2503.
- [10] H. Göksu, H. Burhan, S.D. Mustafafov, F. Şen, *Scientific reports* 10 (2020) 1-8.
- [11] J. Xu, X.T. Yi, T. Zhao, L.Z. Wen, F. Wang, B. Xue, *Mol. Catal.* 511 (2021) 111749-111761.
- [12] S. Ghorbani, R. Parnian, E. Soleimani, *J. Organomet. Chem.* 952 (2021) 122025-122037.
- [13] X. Yao, C. Bai, J. Chen, Y. Li, *RSC Adv.* 6 (2016) 26921-26928.
- [14] F. Gao, Y. Zhang, Z. Wu, H. You, Y. Du, *Coord. Chem. Rev.* 436 (2021) 213825-213848.
- [15] M.T. Räisänen, A. Al-Hunaiti, E. Atosuo, M. Kemell, M. Leskelä, T. Repo, *Catal. Sci. Technol.* 4 (2014) 2564-73.
- [16] C. Parmeggiani, F. Cardona, *Green Chem.* 14 (2012) 547-564.
- [17] X. Wang, X. Zhang, P. Li, K. Otake, Y. Cui, J. Lyu, M.D. Krzyaniak, Y. Zhang, Z. Li, J. Liu, C.T. Buru, *J. Am. Chem. Soc.* 141 (2019) 8306-8314.
- [18] A.R. Judy-Azar, S. Mohebbi, *J. Mol. Catal. A: Chem.* 397 (2015) 158-165.
- [19] B. Li, J. Hong, Y. Ai, Y. Hu, Z. Shen, S. Li, Y. Zou, S. Zhang, X. Wang, G. Zhao, X. Xu, *J. Catal.* 399 (2021) 142-149.
- [20] H. Ghasempour, F. ZareKarizi, A. Morsali, X. W. Yan, *Appl. Mater. Today* 24 (2021) 101157-101166.
- [21] J. Rana, S.T. Sahoo, P. Daw, *Tetrahedron* 99 (2021) 132473.
- [22] L. Geng, M. Zhang, W. Zhang, M. Jia, W. Yan, G. Liu, *Catal. Sci. Technol.* 5 (2015) 3097-3102.
- [23] H.Y. Sun, Q. Hua, F.F. Guo, Z.Y. Wang, W.X. Huang, *Adv. Synth. Catal.* 354 (2012) 569-73.
- [24] S.S. Meng, L.R. Lin, X. Luo, H.J. Lv, J.L. Zhao, A.S. Chan, *Green Chem.* 21 (2019) 6187-6193.
- [25] S. Wang, Z. Zhang, B. Liu, *ACS Sustain. Chem. Eng.* 3 (2015) 406-412.
- [26] E.M. Materón, C.M. Miyazaki, O. Carr, N. Joshi, P.H.S. Picciani, C. J. Dalmaschio, F. Davis, F.M. Shimizu, *Appl. Surf. Sci.* 6 (2021) 100163-100180.
- [27] B.B. Mirjalili, F. Aref, *Res. Chem. Intermed.* 44 (2018) 4519-4531.
- [28] L.M. Rossi, N.J Costa, F.P. Silva, R. Wojcieszak, *Green Chem.* 16 (2014) 2906-33.
- [29] S. Bagheri, F. Pazoki, L. Radfar, A. Heydari, *Appl. Organomet. Chem.* 34 (2020) e5447.
- [30] Q.A. Pankhurst, J. Connolly, S.K. Jones, J. Dobson, *J. Phys. D: Appl. Phys.* 36 (2003) R167.
- [31] S. Shukla, R. Khan, A. Daverey, *Environ. Technol. Innov.* 24 (2021) 101924-101942.
- [32] M. Neamtu, C. Nadejde, V.D. Hodoroaba, R.J. Schneider, L. Verestiuc, U. Panne, *Sci. Rep.* 8 (2018) 1-1.
- [33] M. Munoz, Z.M. De Pedro, J.A. Casas, J.J. Rodriguez, *Appl. Catal B: Environ.* 176 (2015) 249-65.
- [34] Q. Gong, Y. Liu, Z. Dang, *J. Hazard. Mater.* 371 (2019) 677-86.
- [35] S.D. Roy, K.C. Das, S.S. Dhar, *Inorg. Chem. Commun.* 134 (2021) 109050.
- [36] N. Zhu, H. Ji, P. Yu, J. Niu, M.U. Farooq, M.W. Akram, I.O. Udego, H. Li, X. Niu, *Nanomaterials.* 8 (2018) 810-837.
- [37] A. Maleki, *Tetrahedron.* 68 (2012) 7827-33.
- [38] E. Farzad, H. Veisi, *J. Ind. Eng. Chem.* 60 (2018) 114-24.
- [39] L. Kannappan, R. Rajmohan, P. Edwin, *Mater. Lett.* 301 (2021) 130257-130261.
- [40] O. Orgil, E. Schwartz, L. Baruch, I. Matityahu, J. Mahajna, R. Amir, *LWT-Food Sci Technol.* 58 (2014) 571-577.
- [41] B. Singh, J.P. Singh, A. Kaur, N. Singh, *Food Chemistry.* 261 (2018) 75-86.
- [42] E.M. Alexandre, S. Silva, S.A. Santos, A.J. Silvestre, M.F. Duarte, J.A. Saraiva, *Int. Food Res.* 115 (2019) 167-176.
- [43] I. Bibi, N. Nazar, S. Ata, M. Sultan, A. Ali, A. Abbas, et al, *J. Mater. Res. Technol.* 8 (2019) 6115-24.
- [44] B. Şahin, A. Aygün, H. Gündüz, K. Şahin, E. Demir, S. Akocak, *Colloids Surf B: Biointerfaces* 163 (2018) 119-24.
- [45] H. Yang, Y. Ren, T. Wang, C. Wang, *Results Phys.* 6 (2016) 299-304.
- [46] M. Ganeshkumar, M. Sathishkumar, T. Ponrasu, M.G. Dinesh, L. Suguna, *Colloids Surf B: Biointerfaces.* 106 (2013) 208-16.
- [47] L. Sun, C. Huang, T. Gong, S. Zhou, *Mater. Sci. Eng: C.* 30 (2010) 583-9.
- [48] S. Iranfar, M. Hekmati, H. Ziyadi, E. Ghasemi, D. Esmaili, *Inorg. Chem. Commun.* 133 (2021) 108925-108933.
- [49] E.A. Osborne, T.M. Atkins, D.A. Gilbert, S.M. Kauzlarich, K. Liu, A.Y. Louie, *Nanotechnology.* 23 (2012) 215602-215611.